

Insights from digital simulations of sunscreen performance

Sohn, Myriam¹; Herzog, Bernd¹

(1) BASF Grenzach GmbH, Germany

*Dr. Myriam Sohn, Köchlinstrasse 1, 79639 Grenzach-Wyhlen, Germany.
myriam.sohn@basf.com, +49 7624 122673*

Abstract

Background: Computer simulations are frequently used to provide first information about the performance of sunscreens like the sun protection factor (SPF) and the UVA protection factor (UVA-PF) for selected UV-filter combinations. In this paper we show further applications of such simulations.

Methods: UV spectra of current UV filters were measured in emollients of different polarity and the influence on the calculated SPF and UVAPF was assessed. To simulate blue light protection, the spectral range between 400 and 450 nm was considered, and for radical protection a radical action spectrum was employed. For the evaluation of in vitro water resistance data, simulations were used to calculate static and wet SPFs. Finally, the impact of sunscreens on the environment can be calculated by weighting the specific environmental profile of tested UV-filter combination by the UV-protecting efficiency.

Results: The calculated SPF did not depend on emollient polarity, but a slight increase of calculated UVA-PF was observed with more polar emollients. It was also demonstrated that the estimated water-resistance based on the in-vitro absorbance spectrum of tested sunscreen is in good agreement with in vivo results. Furthermore, differences between different filter combinations on the calculated blue light protection, free radical generation protection and impact on the environment can be shown.

Conclusion: In-silico methodology is a powerful tool to screen the effect of an unlimited number of UV-filter combinations, and a large variety of performance criteria can be predicted.

Keywords: sunscreens, in-silico performance, water resistance, blue light, environment

Introduction

First in-silico methodologies for computing the performance of UV-filter combinations were developed beginning 2000s. Such model calculations are based on the simulation of the transmittance of UV light through an applied layer of sunscreen. The simulation requires quantitative UV absorbance data of all UV-filter substances, their photodegradation characteristics, as well as the photointeraction properties between UV-filters, and the oil/water phase repartition synergies. Additionally, a model to describe the irregularity of the film distribution on skin must be considered for the calculations since it is not possible to apply a sunscreen product uniformly due to the irregularity of the skin surface given by the natural skin topography. This is an important consideration, since the transmittance of a sunscreen layer of homogeneous thickness is significantly lower compared to that of an irregular thickness layer of same average thickness. To this purpose, several models were employed. The models evolved in time to provide more accurate predictions starting from a simple two-step film model described by O'Neill [1]. Other models like the calibrated two-step film model [2], the multiple step film model [3], the exponential film model [4], and the continuous height distribution model were developed [5]. In the latter, the gamma law representing an asymmetrical distribution is used to simulate the film thicknesses distribution on skin. A key assumption for using the above-mentioned models to simulate the transmission is the validity of the Beer-Lambert law. Herzog et al. demonstrated that the validity is still given at the UV filter concentrations typically found in the layer of a sunscreen applied on skin [6]. The first model calculations simulated the basic indices of sun and UVA protection factors (SPF & UVA-PF). Simulating the performance of a UV filter combination

became meanwhile the first step of any new suncare product development. Simulations enable an optimization of the UV filter combination before starting laboratory experiments and extensive in vivo performance testing; reducing clinical testing is ethically and economical highly valuable. In this paper, we investigated the relevance and usefulness of computational simulations to predict criteria going beyond the SPF and UVA-PF estimations, such as the assessment of the free radical and blue light protection. Furthermore, we described possible use of simulations to predict the impact of the emollients on the performance or the water resistance of sunscreens.

Computational simulation methods

SPF and UVA-PF predictions

Model calculations for predicting the in silico SPF and in silico UVA-PF indices have been described extensively [2-5,7]. They are based on the same algorithm as for in vitro SPF and in vitro UVA-PF replacing in Eq (1) and (2) the measured transmission by the calculated transmission. The calculation of the transmission of a given UV filter combination requires data of the quantitative UV spectra of all UV-filter substances, their photodegradation characteristics, the photointeraction properties between UV-filters, the oil/water phase repartition synergies and a model to describe the irregularity of the film distribution [7].

$$\text{SPF} = \frac{\sum_{290\text{nm}}^{400\text{nm}} s_{er}(\lambda) \cdot S(\lambda)}{\sum_{290\text{nm}}^{400\text{nm}} s_{er}(\lambda) \cdot S(\lambda) \cdot T(\lambda)} \quad (\text{Eq.1})$$

where, $s_{er}(\lambda)$ is the erythema action spectrum [8], $S(\lambda)$ is the spectral irradiance received from the UV source [9], and $T(\lambda)$ is the light transmittance of the respective UV-filter combination.

$$\text{UVA - PF} = \frac{\sum_{320\text{nm}}^{400\text{nm}} SPPD(\lambda) \cdot SUVA(\lambda)}{\sum_{320\text{nm}}^{400\text{nm}} SPPD(\lambda) \cdot SUVA(\lambda) \cdot T(\lambda)} \quad (\text{Eq.2})$$

where, $SPPD(\lambda)$ is the Pigment Persistent Darkening action spectrum [9], $S_{UVA}(\lambda)$ is the spectral irradiance received from the UVA source [9], and $T(\lambda)$ is the light transmittance of the respective UV-filter combination. The transmittance can be expressed as:

$$T(\lambda) = 10^{-\bar{\varepsilon}(\lambda)\bar{c}d} \quad (\text{Eq.3})$$

where, $\bar{\varepsilon}(\lambda)$ in $(\text{L/mol}^{-1}\cdot\text{cm}^{-1})$ is the average molar absorption coefficient of the UV-filter combination, \bar{c} ($\text{mol}\cdot\text{L}^{-1}$) is the overall molar concentration based on the average molecular weight of the UV-filter combination in the formulation, d is film thickness in cm. The calculation model is based on a continuous film height distribution using the gamma law to simulate the film thickness distribution is an asymmetric distribution and is described by Eq(4):

$$f(h) = \left(\frac{h}{b}\right)^{c-1} \cdot e^{-\left(\frac{h}{b}\right)} \cdot \frac{1}{b \cdot \Gamma(c)} \quad (\text{Eq. 4})$$

where, h is the film height, c is the adjustable shape parameter, b is the normalization parameter, $\Gamma(c)$ is the value of the Γ function. In this model the adjustable shape parameter is calibrated by comparing the calculated SPF to the in vivo SPF of reference formulations.

Protection against free radicals

UV-visible irradiation leads to the generation of free radicals mainly reactive oxygen species in skin [10-12], which initiate a cascade of biological reactions at the molecular level. Free radicals participate to the normal metabolic process, an excess of free radicals generated by an overexposure to UV light may, however, overwork the antioxidant innate defense system and, therefore, may lead to DNA damage and oxidation of endogenous molecules. These impairments will result in long term damages such as skin cancer and premature skin ageing [13-15]. Zastrow and co-workers measured the free radical action spectrum from 280nm up to 700nm and showed that the amount of generated free radicals is wavelength dependent [16]. Considering the wavelength band from 290 to 450nm, UVB (290-320nm), UVA (320-400nm) and blue light (400-450nm) account for 20%, 63% and 18% of generated free radicals, respectively. This underlines the high contribution of UVA rays to the generation of detrimental free radicals in skin. With this action spectrum it becomes possible similarly

to the prediction of the in silico SPF and in silico UVA-PF to simulate the protection index of a specific UV filter combination against the generation of free radicals as given in Eq(5)

$$\text{Free radical protection factor (FR - PF)} = \frac{\sum_{290\text{nm}}^{450\text{nm}} s_r(\lambda) \cdot S(\lambda)}{\sum_{290\text{nm}}^{450\text{nm}} s_r(\lambda) \cdot S(\lambda) \cdot T(\lambda)} \quad (\text{Eq.5})$$

where, $s_r(\lambda)$ is the free radical action spectrum, $S(\lambda)$ is the spectral irradiance, and $T(\lambda)$ is the light transmittance of the respective UV-filter combination. Another way of expressing the protection against free radicals is to provide the percentage of reduction of free radical formation (Eq(6)).

$$\text{Radical reduction (\%)} = 100 - \frac{100}{FR - PF} \quad (\text{Eq.6})$$

To have a comparison, the protection afforded by the different filter combinations against the generation of free radicals was also assessed ex vivo using pig skin. The percentage of free radicals generated after an UV-visible irradiation was measured using electron spin resonance spectroscopy (ESR) for the three formulations. Briefly, in this test the pig skin probe is placed on a filter paper drenched in PBS solution containing a nitroxyl probe as free radical trap. 2 mg/cm² of the tested formulation is applied on the epidermis and a punch biopsy (\varnothing 4 mm) was extracted and placed in a ESR tissue cell. ESR spectrum is recorded before and after UV-visible (360-800nm) irradiation, and the amount of free radicals measured [17].

Blue light protection

The transmittance of Eq(3) can also be calculated for the wavelength band 400 to 450nm to specifically calculate the protection in the blue light range with Eq(7).

$$\text{Blue light protection (\%)} = \left[1 - \frac{\sum_{400}^{450} T(\lambda)}{n} \right] \cdot 100 \quad (\text{Eq.7})$$

where, $T(\lambda)$ is the transmittance at wavelength λ and n is the total number of wavelengths considered between 400 and 450nm.

Impact of emollients on performance

The UV absorbance spectra of the UV filters used for computational simulations generally rely on experimental data of the molar decadic extinction coefficient performed in ethanol. However, solvents used in sunscreens to dissolve solid UV filters and to achieve specific sensorial behavior are lipophilic solvents (generally referred to as emollients). Several studies reported the effect of the polarity of the solvent on the absorbing properties of a UV-filter molecule in terms of absorbance efficiency and bathochromic shift with increased solvent polarity [18-19]. To increase the accuracy of the performance prediction of a UV filter combination, it is, therefore, possible to use for the simulation experimental data of molar decadic extinction coefficients measured in solvents relevant for sunscreens instead of ethanol. Suncare relevant emollients include for instance C12-15 alkyl benzoate, dibutyl adipate, isopropyl myristate either for their good solubilizing power of solid UV filters or their benefit in respect of sensory properties. Using the spectral data obtained in those solvents, respective transmittance data can be calculated and fed into Eq(1) and Eq(2). In that way SPF and UVA-PF values can be calculated for a given UV-filter composition in different emollients [20].

Water resistance calculation

For this application case, the computational simulation was used to calculate the SPF using in vitro transmission measurement of a sunscreen solution to deduce the water resistance of the tested formulation [21]. In this methodology, the sunscreen-covered substrate plates subjected or not to a water immersion step were rinsed off by a solvent mixture to obtain the sunscreen solutions for the status “no water immersion” or “with water immersion”. Two plates were used for each of both conditions. The in vitro absorbance data were then adjusted for dilution for a homogeneous film thickness of 20 µm which provide the extinction per wavelength for the investigated filter combination. The transmittance data for each wavelength are then calculated for an irregular film structure using a gamma law as calculation model to describe the film thickness distribution. The recalculated transmittance data are fed in Eq(1) to calculate the in silico SPF for the status “no water immersion” and “with water immersion” which correspond to the SPF before water immersion and SPF after

water immersion in ISO18861:2020. The percentage of water resistance (WRR) is then calculated from the in silico SPF “before water immersion” and in silico SPF “after water immersion” as given in Eq(8).

$$\text{WRR (\%)} = \frac{\text{in silico SPF before water immersion}-1}{\text{in silico SPF after water immersion}-1} * 100 \quad (\text{Eq.8})$$

Results and discussion - simulation examples

SPF, UVA-PF, free radical, and blue light protection

Table 1 provides the performance simulations of three filter combinations with an in silico SPF of 30 but differing in the photostability and quality of their UVA protection. The relative amounts (%) of free radicals measured ex vivo are also given in Table 1. All combinations were formulated in the same O/W emulsion chassis. The filter concentrations are given as active amount.

Table 1. Performance simulations including free radical and blue light protection of three filter combinations differing in UVA protection

Characteristic	Partly stabilized UVA protection	Photostable UVA protection	Photostable and long-wave UVA protection
Formulation ID	17-214-1-1	17-214-1-2	17-214-1-3
Filter system	5% EHS 2% EHT 2% PBSA	5% EHS 4% EHT 1,5% TBPT	3,5% EHS 0,5% EHT 1,5% TBPT
Broad-spectrum	2,5% BEMT	2,2% BEMT	1% BEMT 4% MBBT
UVA	4% BMDBM	4% DHHB	4% DHHB

SPF	In silico SPF	30	30	30
	In vivo SPF	-	-	34 ± 4.3
	(n= 5)			
UVA-PF	In silico	10	11	28
	UVA-PF			
	In vitro	-	10	25
	UVA-PF			
Free radicals	Calculated radical reduction (%)	79%	87%	95%
	Free radicals produced ex vivo (%)	30 ± 8%	24 ± 4%	10 ± 5%
	(Reduction of free radicals, %)	(70%)	(76%)	(90%)
	Blue light protection (%), calculated	2%	6%	65%

EHS, Ethylhexyl Salicylate; EHT, Ethylhexyl Triazone; PBSA, Phenylbenzimidazol Sulfonic Acid; BEMT, Bis-Ethylhexyloxyphenol Methoxyphenyl Triazine; BMDBM, Butyl Methoxydibenzoylmethane; DHHB, Diethylamino Hydroxybenzoyl Hexyl Benzoate; MBBT, Methylene Bis-Benzotriazolyl Tetramethylbutylphenol ; TBPT, Tris-Biphenyl Triazine

The in silico SPF of all combinations equaled 30, we measured the in vivo SPF of the “photostable and long UVA” combination which was in good agreement with the prediction. Also, the measured UVA-PF in vitro was in good agreement with the simulated values for “photostable UVA” and “photostable and long UVA” combinations, confirming the

suitability of using simulations for predicting the basic SPF and UVA-PF indices. The three UV filter combinations were also evaluated in respect of their efficacy to protect against the formation of free radicals following UV exposure. According to the radical action spectrum, the UVA part plays a major role in the generation of free radicals. Sunscreen products generally exhibit a certain level of UVA protection; in Europe, the commission recommendation of 2006 recommends a minimum UVA-protection factor that equals at least one third of the SPF value [23], which corresponds to the protection afforded by “partly stabilized UVA” and “photostable UVA” combinations in Table 1. Whereas there is a recommendation for a minimum UVA protection for sunscreen products, there is no instructions for instance for day care products with UV protection. Around 10% of launched day care products in Europe during last year exhibited a SPF value; half of them with a SPF value higher than 25 [23]. Since UVA irradiation intensity is more stable during the year and time of the day than UVB irradiation, and that UVA rays penetrate glass from windows, a minimum and photostable UVA protection in day care is as important as if not more than in suncare.

The simulation of the protection against the generation of free radicals of the three filter combinations showed that 79% of the theoretical free radicals generated under UV are reduced with the “partly stabilized UVA” combination and 87% with the “photostable UVA”. The increase of the UVA protection in “photostable and long-wave UVA” compared to the two other combinations allowed to achieve a balanced protection over the full UVB and UVA range, indeed the UVA-PF value is close to the SPF value. A UVA-PF value that approximates a SPF value means that the quantity of absorbed UV light is reduced homogeneously and the proportion of the UV achieving the skin is similar to the natural light. This boosted UVA protection enabled a reduction by 95% of the free radicals theoretically generated. From the three UV filter combinations “partly stabilized UVA” was the less effective in protecting against the production of free radicals in skin, “photostable UVA” provided a better protection. The “Photostable and long-wave UVA” was the most effective in protecting against the generation of free radicals in skin. The ex vivo results are in good agreement with the simulations indicating the suitability of the simulations. An effective protection against the UV-induced free radicals requires a photostable and long-wave UVA protection.

Impact of emollients

Figure 1 displays the absorbance profile of EHT a UVB filter, BEMT a broad-spectrum (B-S) filter and DHHB a UVA filter in three relevant suncare emollients C12-15 alkyl benzoate, dibutyl adipate, and isopropyl myristate. C12-15 alkyl benzoate and dibutyl adipate are classified as polar emollients whereas isopropyl myristate is medium polar. The value of specific extinction $E(1,1)$ is the absorbance for a 1% (w/v) solution at an optical thickness of 1cm.

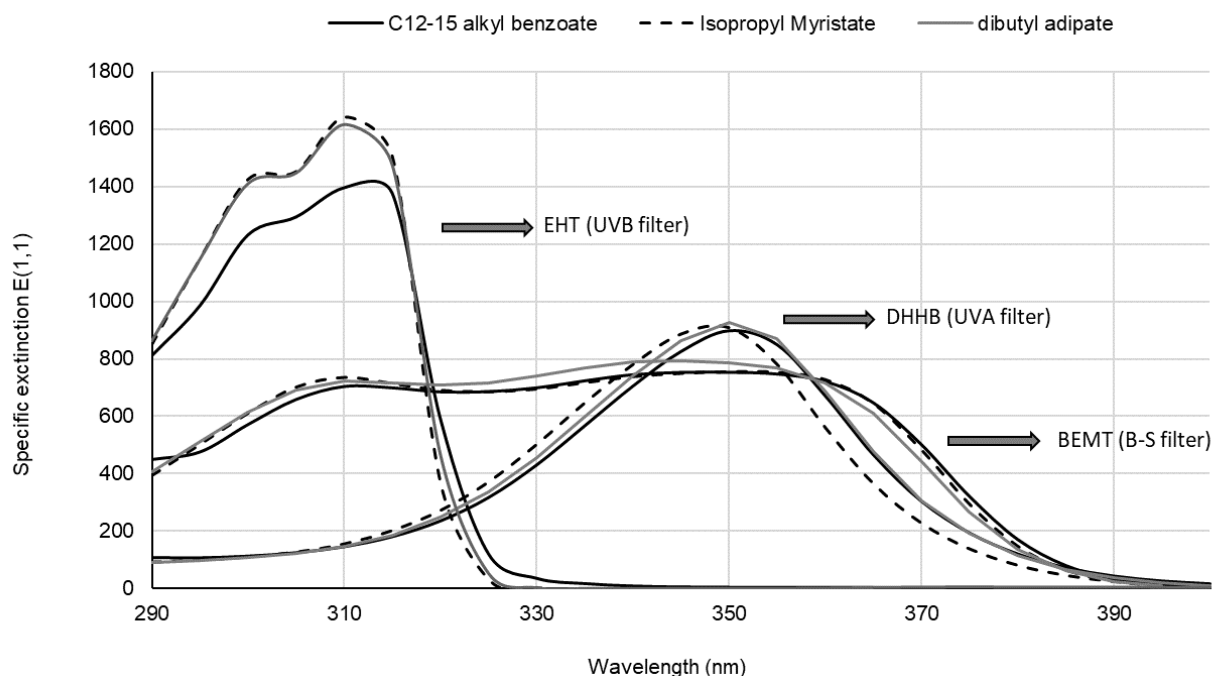


Figure 1. UV absorbance spectra of EHT, DHHB and BEMT dissolved in C12-15 alkyl benzoate, dibutyl adipate, and isopropyl myristate

At a first glance, Figure 1 shows that the absorbance profiles of the three filters in the three emollients were relatively similar except for EHT in C12-15 alkyl benzoate which appeared to be quite lower than for EHT in dibutyl adipate and isopropyl myristate. This difference can not be attributed to the polarity since C12-15 alkyl benzoate with a lower performance and dibutyl adipate with a higher performance are both polar, whereas the absorbance in

isopropyl myristate which is medium polar was as high as in dibutyl adipate. For the UVA filter DHHB, the two polar emollients showed a bathochromic shift. Finally, the emollients nearly showed no effect on the absorbance profile of the broad-spectrum filter BEMT.

Further, to evaluate the significance on the performance of the slight differences in the absorbance profiles, the SPF and PPD values of a filter combination were calculated using the absorbance data measured for each lipophilic UV-filter – emollient system. The filter combination consisted of 10% Diethylamino Hydroxybenzoyl Hexyl Benzoate, 2,5% Bis-ethylhexyloxyphenol Methoxyphenyl triazine, 3% Ethylhexyl Triazone, and 2,5% Tris Biphenyl Triazine. The results and deviation as determined in [16] are shown in Figure 2 for four different solvents.

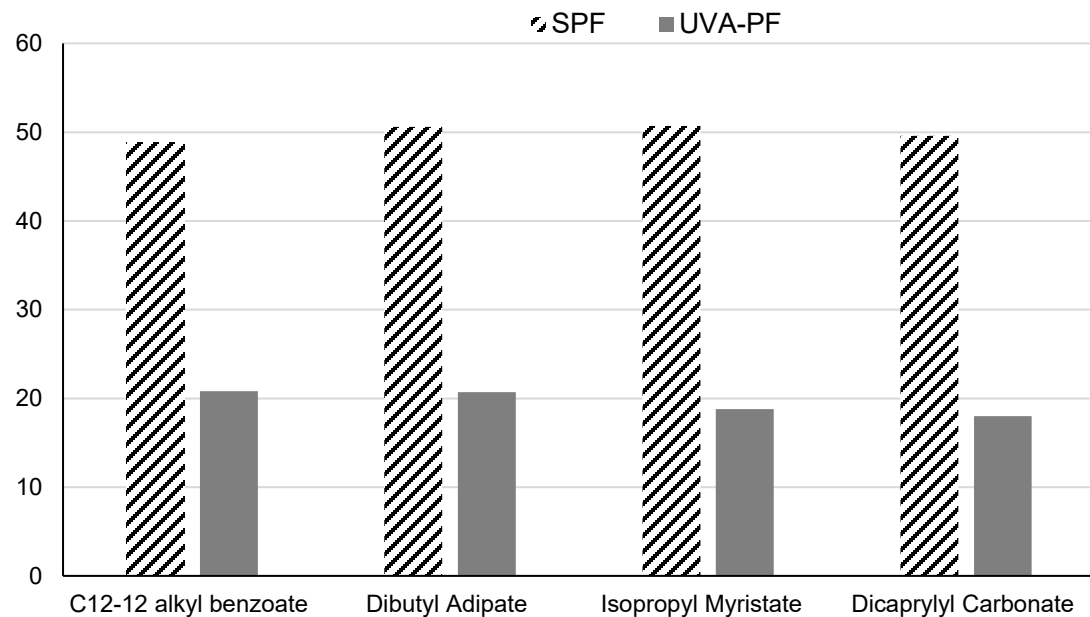


Figure 2. *in silico* SPF and *in silico* UVA-PF in dependence on the solvent (UVAPF simulation based on persistent pigment darkening)

It is noticeable from Figure 2 that the solvent had only minor effect on the SPF value of evaluated filter combination, with a maximum difference of 3,7% between the highest and lowest in silico SPF equaling 50,7 and 48,8 for isopropyl myristate and C12-15 alkyl benzoate, respectively. The difference noticed in the absorbance profile of EHT in C12-15 alkyl benzoate did not result in extreme differences in the in silico SPF value. In comparison, the effect of emollients was slightly more observable in the in silico UVAPF values and was related to the polarity. In Figure 2 the in silico UVAPF decreases with the decrease of the polarity of the solvent achieving a maximum difference of 13% between the highest and lowest in silico UVAPF; 20,8 and 18 for C12-15 alkyl benzoate and dicaprylyl carbonate, respectively. Indeed, the increase in polarity of the solvent resulted in a bathochromic shift of the absorbance spectrum; the excited state of DHHB is presumably more polar than its ground state and is better stabilized by polar solvents, the energy needed for the electron delocalization in the molecule is reduced. This bathochromic shift seems to be expressed in the in silico UVAPF value of investigated UV-filter combination. Even though the effect was rather small, considering the emollients in the calculation of the performance indices may increase the accuracy of the prediction.

Water resistance calculation

We assessed the water resistance of three O/W sunscreens with the UV-filter compositions as given in Table 2. The formulation chassis was the same for the three sunscreens which differed in the filter system in particular in the amount of the water soluble UV filter PBSA. The in vitro absorbance data were mathematically handled as described above and more detailed in [20] to obtain the calculated values of transmittance through an irregular film for tested sunscreen. The in silico SPF with and without water immersion were calculated with the simulation tool making use of the calculated transmittance and are reported in table 2 together with the deduced WRR (%).

Table 2. UV filter compositions of investigated sunscreens, in silico SPF and WRR(%)

Formulation ID	1	2	3	
Filter system	UVB 3% EHT 3% PBSA 5% EHS 5% DBT	3,5% EHT 1,5% PBSA 2,5% BEMT 2% BEMT Aq 8% DHHB	3% EHT 5% EHS 3% BEMT 2,5% BEMT Aq 8% DHHB	3% BEMT 2,5% BEMT Aq 6% DHHB
In silico SPF	no water immersion with water immersion	37 12	48 29	58 47
WRR (%)	31%	60%	81%	

DBT, Diethylhexyl Butamido Triazole, BEMT Aq corresponds to the active amount of BEMT when using the market product Tinosorb S Lite Aqua.

The water resistance increased with a decrease in the concentration of the water soluble UVB filter PBSA. This result appears reasonable. The presence of the dispersed BEMT in water had no negative impact on the water resistance since formulation 3 was water resistant. The calculation of the WRR may be useful to screen a series of formulations to test the impact of a certain change such as a different filter system as in Table 2, but also the exchange of a raw material, the impact of a water resistant agent, or a different formulation base.

Conclusions

Computational simulations for predicting the performance of sunscreens rely on the calculation of the transmission. These data can, afterwards, be used for different purposes besides the estimation of standard SPF and UVA-PF factors. In this paper we described the use of calculations to predict the protection against blue light and against the generation of free radicals, which can be optimized with the appropriate filter selection. Further, we used the simulations to assess the effect of emollients commonly used in sunscreens on the performance of UV filters, which revealed not to be very strong. Calculations of sunscreen performance have been shown to be extremely useful in the design of new sunscreen formulations. Digital methodologies are fast, unlimited in the number of calculations, economical and ethical valuable.

Conflict of Interest: NONE

References

- [1] O'Neill JJ. Effect of film irregularities on sunscreen efficacy. *J Pharm Sci* 73 (1984) 888-891
- [2] Herzog B. Prediction of sun protection factors by calculation of transmissions with a calibrated step film model. *J Cosmet Sci.* 53 (2002)11-26
- [3] Tunstall DF. A mathematical approach for the analysis of in vitro sun protection factor measurements. *J Cosmet sci* 51 (2000) 303-315
- [4] Herzog B. Prediction of sun protection factors and UVA parameters by calculation of UV transmissions through sunscreen films of inhomogeneous surface structure. In “Sunscreens-regulation and commercial development”, ed. Nadim Shaath, 3rd ed., Taylor & Francis, Boca Raton (2005)
- [5] Ferrero L. et al. Efficiency of a continuous height distribution model of sunscreen film geometry to predict a realistic sun prtoection factor. *J Cosmet Sci* 54 (2003) 463-481
- [6] Herzog B. On the validity of Beer Lambert law and its significance for sunscreens. *Photochem Photobiol* (2017)
- [7] Herzog B., Osterwalder U. Simulation of sunscreen performance. *Pure Appl Chem* 87 (2015) 937–951
- [8] ISO 24444:2010 - Cosmetics - Sun protection test methods - In vivo determination of the sun protection factor (SPF). (2010).
- [9] ISO 24443:2012 - Determination of sunscreen UVA photoprotection in vitro. (2012).
- [10] Tyrrell R. Ultraviolet radiation and free radical damage to skin. *Biochem Soc Sym* (1995) 61:47-53
- [11] Ogura et al. Mechanism of lipid radical formation following exposure of epidermal homogenate to ultraviolet. *J Invest Dermatol* (1991) 97(6):1044-1047
- [12] Baier et al. Direct detection of singlet oxygen generated by UVA irradiation in human calles and skin. *J Invest Dermatol* (2007) 1498-1506
- [13] Krutmann J. Ultraviolet A radiation-induced biological effects in human skin: relevance for photoageing and photodermatoses. *J Dermatol Sci* (2000) 23:22-26
- [14] Kelfkens G. et al. Tumorigenesis by short-wave ultraviolet-A – papilomas versus squamous cell carcinomas. *Carcinogenesis* (1991)12(8):1377-1382

- [15] Marrot L., Meunier J-R. Skin DNA photodamage and its biological consequences. *J Am Acad Dermatol* (2001) 10(8):139-148
- [16] Zastrow et al. The missing link – light induced (280-1600 nm) free radical formation in human skin. *Skin Pharmacol Physiol* (2009) 22:31-44
- [17] Sohn et al. Impact of photostability and UVA/UVA-blue light protection on free radical generation. *SÖFW* (2019) 145
- [18] -Agrapidis-Paloypis et al. The effect of solvents on the ultraviolet absorbance of sunscreens. *J. Soc. Cosmet. Chem.* (1987) 38:209-221
- [19] Shaath, N.A. On the theory of ultraviolet-absorption by sunscreen chemicals. *J Soc. Cosmet. Chem.* (1987) 38:193-207
- [20] Sohn et al. Effect of emollients on UV filter absorbance and sunscreen efficiency. *J Photochem Photobiol B* (2020) 205:111818.1–8
- [21] [3] Sohn M. et al. In vitro water resistance testing using SPF simulation based on spectroscopic analysis of rinsed sunscreens. *Int J Cosmet Sci* (2018) 40:217–225
- [22] Commission recommendation of 22 September 2006 on the efficacy of sunscreen products and claims made relating thereto. <https://eur-lex.europa.eu/LexUriServ/LexUriServ.do?uri=OJ:L:2006:265:0039:0043:en:PDF>, accessed June 2022
- [23] Mintel, Global new products database (GNPD) Personal Care portal, Search criteria: Face/Neck care, mai 2021-mai 2022, Europe, without and with SPF indication. Available at <http://www.gnpd.com/> Restricted access. Accessed June 2022